


Age-dependent patterns of spatial autocorrelation in fish populations

JONATAN F. MARQUEZ ^{1,5}, BERNT-ERIK SÆTHER,¹ SONDRÉ AANES,² STEINAR ENGEN,³ ARE SALTHAUG,⁴ AND
ALINE MAGDALENA LEE ¹

¹Centre for Biodiversity Dynamics, Department of Biology, Norwegian University of Science and Technology, 7491 Trondheim, Norway

²Norwegian Computing Center, 0314 Oslo, Norway

³Centre for Biodiversity Dynamics, Department of Mathematical Sciences, Norwegian University of Science and Technology, 7491 Trondheim, Norway

⁴Institute of Marine Research, Postbox 1870 Nordnes, 5817 Bergen, Norway

Citation: Marquez, J. F., B.-E. Sæther, S. Aanes, S. Engen, A. Salthaug, and A. M. Lee. 2021. Age-dependent patterns of spatial autocorrelation in fish populations. *Ecology* 00(00):e03523. 10.1002/ecy.3523

Abstract. The degree of spatial autocorrelation in population fluctuations increases with dispersal and geographical covariation in the environment, and decreases with strength of density dependence. Because the effects of these processes can vary throughout an individual's lifespan, we studied how spatial autocorrelation in abundance changed with age in three marine fish species in the Barents Sea. We found large interspecific differences in age-dependent patterns of spatial autocorrelation in density. Spatial autocorrelation increased with age in cod, the reverse trend was found in beaked redfish, while it remained constant among age classes in haddock. We also accounted for the average effect of local cohort dynamics, i.e. the expected local density of an age class given last year's local density of the cohort, with the goal of disentangling spatial autocorrelation patterns acting on an age class from those formed during younger age classes and being carried over. We found that the spatial autocorrelation pattern of older age classes became increasingly determined by the distribution of the cohort during the previous year. Lastly, we found high degrees of autocorrelation over long distances for the three species, suggesting the presence of far-reaching autocorrelating processes on these populations. We discuss how differences in the species' life history strategies could cause the observed differences in age-specific variation in spatial autocorrelation. As spatial autocorrelation can differ among age classes, our study indicates that fluctuations in age structure can influence the spatio-temporal variation in abundance of marine fish populations.

Key words: age segregation; age structure; age truncation; Barents Sea; cohort dynamics; cohort spatial distribution; dispersal; life stage; spatial autocorrelation; spatial dynamics; spatial variance.

INTRODUCTION

Population dynamics are regulated by time- and space-varying density-dependent and density-independent factors that differentially affect individuals within a population (Gamelon et al. 2016, Engen et al. 2018a). Despite the high degree of heterogeneity within most ecosystems, populations often exhibit spatial autocorrelation in their dynamics, meaning that temporal variations in local abundances are correlated in space, with nearby locations generally having more similar fluctuations in abundance than distant locations (Liebhold et al. 2004). Three mechanisms are known to cause spatial autocorrelation in population fluctuations. Increased dispersal can homogenize local population abundances, increasing autocorrelation in highly mobile species or across highly conductive landscapes (Lande et al. 1999). For example, bird populations tend to be more spatially

autocorrelated across farmlands compared with conspecifics living in woodlands where trees might pose limitations to dispersal (Paradis et al. 1999). Even without dispersal, populations can become spatially autocorrelated over large distances when subjected to common density regulatory and spatially synchronous environmental factors such as temperature or precipitation, (Moran 1953, Tedesco et al. 2004, Engen and Sæther 2005, Hansen et al. 2020). Trophic interactions can also promote spatial autocorrelation (Jarillo et al. 2020), for example through the presence of a nomadic predator regulating the vital rates of a prey population (Ims and Andreassen 2000, Vasseur and Fox 2009). In addition, because density regulatory processes influence dispersal rates and abundance dynamics, differences in density regulation among species and across time and space can influence spatial autocorrelation patterns (Lande et al. 1999, Walter et al. 2017, Marquez et al. 2019).

Age classes within a population often also differ in some of the processes that affect spatial autocorrelation at a population level, such as dispersal, density regulation, habitat preference, environmental sensitivity, and/or trophic interactions (Berkeley 2004, Planque et al. 2011).

Manuscript received 1 February 2021; revised 28 May 2021; accepted 21 June 2021. Corresponding Editor: Lorenzo Ciannelli.

⁵E-mail: jonatan.fredricson@gmail.com

In fish, these differences can result in distinct spatial distributions among age classes (Planque et al. 2011), but little is known about how age-specific characteristics might influence age-specific spatial autocorrelation patterns. Some studies have shown that reductions in the mean age of a population (i.e. age truncation), caused by size selective harvesting, can increase heterogeneity in the spatial distribution of abundance (Kuo et al. 2016, Wang et al. 2020). Higher spatial heterogeneity, similar to lower spatial autocorrelation, may indicate more aggregations across space (Reuman et al. 2017). Therefore, reductions in mean population age could be expected to lower its degree of spatial autocorrelation. However, our understanding of the processes linking age structure and spatial variance remains unclear. Some researchers have hypothesized that different ages have different spatial variance patterns due to age-specific characteristics, while others have hypothesized that changes in age structure might induce changes in the spatial organization of the remaining population. For example, Kuo et al. (2016) argued that, because younger age classes are subject to stronger density-dependent dynamics and older age classes tend to better tolerate adverse environmental conditions (Gamelon et al. 2016), the loss of old age classes increases the overall strength of density dependence, and therefore the degree of spatial heterogeneity. Alternatively, the removal of larger individuals could also increase the spatial aggregation of the rest of the population and reduce dispersal, thereby also increasing spatial heterogeneity (Jenkins et al. 2007, Kuo et al. 2016). Wang et al. (2020) compared age diversity to spatial variance and suggested that populations whose life stages inhabit distinct regions spread potential risks across habitats, buffering against local resource variation and increasing overall spatial homogeneity. In contrast, Hsieh et al. (2008) argued that reduced mean population age could cause contraction in the geographical distribution of a population, which could increase the sensitivity of the entire population to one key environmental variable over a large geographical region, thus increasing spatial homogeneity (Berkeley 2004).

Local density of a cohort can be temporally autocorrelated, i.e. local density of the cohort one year is correlated with the local density of the cohort in the previous year. This correlation can be caused by base local mortality rates coupled with processes such as homing behavior, memory coupled with social learning (i.e. entrainment of young by older individuals), site fidelity, or size-dependent changes in habitat preference that result in constant local dispersal rates (Planque et al. 2011, Nielsen and Seitz 2017). Because of this temporal autocorrelation, part of the spatial autocorrelation pattern in the density of an age class can be related to processes affecting the densities of younger age classes, which are being carried over in time by the cohort. We can quantify some of these carried-over spatial density patterns by estimating the expected local density of an age class based on the local density of the cohort in the

previous year. Differences between expected and the observed local densities are assumed to represent unexplained density variation associated with processes acting within one age class, from this point forwards referred to as cohort-independent density. Spatial autocorrelation in cohort-independent density could then help the separation of spatially autocorrelating processes affecting a cohort throughout its life from those affecting the latest age class (Lindström and Kokko 2002). For example, if the density of an age class is spatially autocorrelated, but the cohort-independent density is not, we can assume that the spatial density pattern is mostly determined by the cohort density in previous years. This could happen when individuals become strongly anchored to a preferred area. In contrast, if the cohort-independent density is also spatially autocorrelated, the dynamics of that age class are probably more sensitive to spatially autocorrelating processes affecting that age class particularly, and independent from processes autocorrelating the cohort in previous age classes.

Understanding how different processes affect spatial autocorrelation in population fluctuations is crucial in ecology because spatial autocorrelation influences important ecological processes, such as extinction probability (Heino et al. 1997), vulnerability to disease outbreaks (Ovaskainen and Cornell 2006), maximum sustainable yield (Engen 2017, Engen et al. 2018b), and sensitivity to climate variability (Hanski and Woiwod 1993). Similarly, variation in age structure influences population dynamics and risk of extinction (Gamelon et al. 2016). Here we analyze how spatial autocorrelation in fluctuations of abundance vary with age or life stage in three species of marine fish inhabiting the Barents Sea: cod (*Gadus morhua*), haddock (*Melanogrammus aeglefinus*), and beaked redfish (*Sebastes mentella*). Here, we characterize the spatial autocorrelation through three key parameters. First, the degree of autocorrelation as the distance approaches zero, which can be important for understanding the influence of local impacts on neighboring regions and vice versa. Second, the spatial scale of the autocorrelation, defined as the standard deviation of the autocorrelation function, shows how localized or globalized are density dynamics and highlights the potential risks of local or global extinctions within a population (Engen et al. 2002b). Third, the degree of autocorrelation at “infinity”, i.e. the value that the autocorrelation approaches as distances become very long, which can provide information about a process affecting the entire population, and is biologically crucial because changes in that process could put the entire population at risk of extinction.

METHODS

Study area and species

We used spatial bottom-trawl survey data on three species of marine fish found in the Barents Sea: cod

(*Gadus morhua*), haddock (*Melanogrammus aeglefinus*) and beaked redfish (*Sebastes mentella*). Important inter-specific differences in life history, behavior, diet, spatial distribution, and phenology, among other key ecological characteristics, have been reported previously for the three study species (e.g. Albikovskaya and Gerasimova 1993, Olsen et al. 2010, Bjørkvoll et al. 2012). The three species use the Barents Sea as a nursery and feeding ground, although reports on international commercial catches have also suggested that a proportion of the adult beaked redfish population's spatial distribution extends into the north-east Atlantic ocean, and outside our sampling area (ICES 2020). Mature individuals carry out annual migrations to spawn (cod and haddock), and extrude larvae (beaked redfish), along the western Norwegian coast and outside our study region, while oceanic currents transport the eggs and larvae of the three species back into the Barents Sea (Olsen et al. 2010, Drevetnyak et al. 2011, Planque et al. 2013). Spawning take place primarily between March to April for cod and beaked redfish, and April to early May for haddock (Olsen et al. 2010, Planque et al. 2013). The timing of the spawning coincides, to some degree, with the survey period, therefore part of the adult portion of the population is unaccounted for. The sea is highly seasonal, with a sea ice layer covering a large area during winter, before gradually melting northward and eastward during the spring months. The hydrology of the region is influenced by three main current systems: the Norwegian coastal current and the North Atlantic current, which flow from the south-west bringing warmer waters, and the Arctic current, which flows in from the north-east bringing colder waters. While primary productivity is present across the entire Barents Sea, the mixing of the water masses in an area of the Barents Sea called the Polar (or Arctic) front, coupled with the retreating sea ice during spring, results in highly variable peaks of primary productivity (i.e. algae blooms) that attract high numbers of individuals from several fish species (Loeng and Drinkwater 2007).

The younger stages of the three study species feed mainly on plankton (Dalpadado et al. 2009), but shift their diet as they grow. Cod shifts to a general fish-dominated diet by age three or four, which includes cannibalisms of younger age classes, becoming a key top predator in the Barents Sea ecosystem (Olsen et al. 2010). Juvenile haddock adopt a diet centered on benthic organisms upon settling, with other prey only appearing occasionally in their diet (Dolgov et al. 2011). Beaked redfish is regarded as a planktivore throughout its life, although larger individuals are known to feed on small fish and squid (Albikovskaya and Gerasimova 1993). The three species are subject to harvesting, with redfish currently recovering from poor stock levels caused by low recruitment between 1998 to 2005 (ICES 2019).

Age of maturation varies among years and among individuals for the three study species but, on average,

50% of the population will have reached maturity by the ages of 7 for cod, 6 for haddock and 11 for beaked redfish (ICES 2020). Upon reaching maturity, individuals start to migrate annually to their spawning grounds. We used these ages as thresholds to differentiate the mostly reproductive immature and mostly reproductive mature life stages of the population. For simplicity we will from this point forwards refer to the individuals from the immature and mature stages as juveniles and adults, respectively.

Field survey

The population spatial autocorrelations were estimated using data from scientific bottom-trawl surveys performed annually by the Norwegian Institute for Marine Research and the Polar Research Institute of Marine Fisheries and Oceanography from January to March, from 1985 to 2016 (Jakobsen et al. 1997, Aanes and Vølstad 2015). The trawl survey was spatially stratified and sampled locations were approximately uniformly distributed in space. The survey has been mostly standardized with respect to sampling gear and performance, except for a reduction in the mesh size of the codend from 35-40 mm to 22 mm in 1994 to prevent potential sampling size bias among 1-year-old cod and haddock. For more details on sampling protocols see Jakobsen et al. (1997), Johannesen et al. (2009), Fall et al. (2020). The fish were sampled onboard, following the instructions given in Mjanger et al. (2020) and otoliths were collected to determine the age of the individuals (Johannesen et al. 2009, Mehl et al. 2016). When the catch was so large that length-measuring the entire catch was unfeasible, a representative random subsample was measured. From this subsample, otoliths to age the fish were collected for an extra subsample of the fish, following a length-stratified sampling design. Before 1993, five individuals per 5 cm length group were aged for a spatially stratified subset of trawls, from 1993 to 1995 only two individuals per 5 cm length group were aged, but for a larger subset of trawls. Since 1996, one individual per 5 cm length group has been aged in all trawls. Lastly, the collected data were then used to make age-length keys to raise or extrapolate the age distribution of each catch. In total, 8,288 trawls were performed, in which 7,037 contained haddock, 8,145 contained cod, and 5,153 contained beaked redfish.

Data analysis

The study region was subdivided using a grid with hexagonal cells because this shape homogenizes the distances between centroids of neighboring cells. The resolution of the grid can influence the outcome of the analyses by, for example, resulting in a high number of cells with incomplete time series at finer resolutions or failing to capture the spatial pattern at too coarse resolutions. To assess the effects of the resolution, the analyses

were repeated using grid cell sizes of 2,500, 3,600, 4,900, 6,400, 8,100, 10,000, and 12,100 km² (see Appendix Fig. S1, S2). The results presented here corresponded to a grid cell size resolution of 6,400 km² because finer resolutions gave similar results and coarser resolutions increased the uncertainty in the estimates. In addition, the analysis was repeated after shifting the hexagonal grid 15 times along the latitudinal and longitudinal gradients. This resulted in slight differences in how samples were grouped to average cell densities, preventing grid cells with fewer samples from generating outliers that could cause biases in the results.

Densities (N_t) per grid cell (i.e. local densities) were estimated by, first, dividing the number of individuals caught by the area swept by the trawl (c.f. Aanes and Vølstad 2015), second, matching the estimated density of each sampling event to the corresponding grid cell and, third, calculating the average within each grid cell and year. We calculated the average local densities of (1) individuals of each species, (2) individuals of each life stage and species, (i.e. juveniles and adults, based on the age of 50% maturity), and (3) individuals of each age (ages 1–8) of haddock and cod. Because the distribution ranges of the three species varied in extent within the study region, we only included grid cells that had at least one recorded presence of the species. The density estimates (+1) were log-transformed ($=\mathbf{Y}$) to normalize their distribution and preserve zeros. We then centered the density estimates of each cell across years ($\mathbf{y} = \mathbf{Y} - \bar{\mathbf{Y}}$) and scaled the centered density estimates of each gridded cell across years using the standard deviation (i.e. $\sqrt{\sum(\mathbf{y}^2)/(n-1)}$); where \mathbf{y} is the vector with all centered densities for a given cell, and n is the number of years that site was surveyed.

In addition, we estimated cohort-independent density. For this, we first estimated the expected local densities based on the local densities of the cohort in the previous year as the predictor by fitting the following generalized linear model:

$$Y_{a,s,t} = \alpha_{a,s} + \beta_{a,s} \times Y_{a-1,s,t-1}, \quad (1)$$

where the density of an age class (a) at site s and year t , $Y_{a,s,t}$, is dependent on an intercept for each age and each site, $\alpha_{a,s}$, plus the regression coefficient for each age and site, $\beta_{a,s}$, multiplied by the density of 1-year-younger individuals in the same site and in the previous year, $Y_{a-1,s,t-1}$. This model assumes a constant age-specific base mortality and migration rate for each site. In reality, these processes might be more dynamic, but we expected this simplification to capture the main effects, assuming no permanent or persistent changes within the habitat range (e.g. significant changes in oceanic currents, habitat destruction) (Quinn and Deriso 1999). Residuals from this model represented local variation in the density of individual age classes after removing the expected cohort effects, and therefore assumed to be more strongly related to processes affecting that age

during the same year. These residuals are from this point forwards referred to as cohort-independent density. The cohort-independent density was scaled across years by the standard deviation, in the same way that the density estimates were scaled and standardized.

We estimated the spatial autocorrelation in density and cohort-independent density parametrically using a model that assumed the data to be dependent in space but independent in time (Engen et al. 2005, Grøtan et al. 2005). The model described the centered and scaled densities (y) or the cohort-independent density (i.e. residuals from fitting Eq. 1), from this point forwards jointly noted as X , at site s and time t as:

$$X(s, t) = \kappa(s) + W(s, t) + \varepsilon(s, t) \quad (2)$$

where $\kappa(s)$ is the mean at site (s), and $W(s, t)$ and $\varepsilon(s, t)$ are spatially dependent and spatially independent random variables, respectively, with zero means. The spatially dependent variable $W(s, t)$ describes the spatially structured deviations from the mean, while $\varepsilon(s, t)$ accounts for the residual variability associated with local variation and sampling variability. The covariance function describing how the spatially structured deviations from the mean vary with distance (d) is written as

$$C_w(d) = \text{Cov}(W(s, t), W(r, t)) = \sigma(s)\sigma(r)\rho_X(d) \quad (3)$$

where the covariance between any two sites (s and r) depends on the variance σ^2 at sites s and r , and the spatial autocorrelation ρ given the distance d between them. The spatial autocorrelation function is

$$\rho(d) = \rho_\infty + (\rho_0 - \rho_\infty)h(d) \quad (4)$$

in which ρ_0 and ρ_∞ are the correlations among densities as distance approaches zero and infinity, respectively, while $h(d)$ is a Gaussian function, $\exp\left(-\frac{d^2}{2l^2}\right)$, describing how correlation decays with increasing distance, where l represents the spatial scaling and corresponds to the distance at one standard deviation of the autocorrelation function (Lande et al. 1999). The higher the l parameter, the slower the rate of decrease in autocorrelation with increasing distance, highlighting the presence of processes acting across greater distances.

Lastly, writing $\mathbf{X}_t = (X(S_1, t), X(S_2, t), \dots, X(S_{n_s}, t))'$, with n_s being the number of sites, we get $E(\mathbf{X}_t|\boldsymbol{\kappa}) = \boldsymbol{\kappa}$ and $\text{Var}(\mathbf{X}_t|\boldsymbol{\kappa}) = \boldsymbol{\Sigma} + \sigma_\varepsilon^2 \mathbf{I}$, where $\boldsymbol{\Sigma}$ corresponds to the covariance among sites at time t and $\sigma_\varepsilon^2 \mathbf{I}$ is the variance of the spatially independent variables. If we then assume that both the spatially structured deviations from the mean W and the residual variability ε are log-normally distributed, the mean corrected values should be multivariate normally distributed, allowing the likelihood function to estimate the parameters ρ_0 , ρ_∞ , and l through numerical optimization. The distributions of

the parameters are obtained by parametric bootstrap, where the model is fitted to simulated datasets generated by drawing random numbers from a multivariate normal distribution defined by the parameters ρ_0 , ρ_∞ , and l estimated with the original data. The standardized parameters produced using this approach promote comparison within and between species, and can be linked to a solid body of theoretical work (Grøtan et al. 2005, Engen 2017).

For simplicity, spatial autocorrelation analyses were performed assuming isotropic autocorrelation decay. There is a chance that spatial heterogeneity in the region could be causing autocorrelation to decay at different rates toward different directions from specific locations, but this would be unlikely to result in consistent patterns that would cause systematic biases in the estimates. All data analyses were carried out in R version 4.0.0 (R Core Team 2020; see Data S1).

RESULTS

Spatial distribution

The three species showed some differences in their geographic affinities within the Barents Sea and changes in their distribution with age. Cod were spatially age segregated. Young cod were found across most of the Barents Sea but in highest densities around the north and east Barents Sea, i.e. in the Polar front region (Fig. 1a). The density peak area of cod gradually shifted toward the center and then southwest of the Barents Sea with increasing age, while also becoming increasingly absent in the eastern Barents Sea. All ages of haddock were found in higher densities around the warmer south and southwest of the Barents Sea, and became increasingly absent in the north-eastern half of the Barents Sea with age (Fig. 1a). Beaked redfish were located within a smaller area than cod and haddock, mostly coinciding with deeper regions (Fig. 1b). As juveniles, beaked redfish were rather homogeneously spread, although their density peaked in the center of the range within which they were found (Fig. 1b). As adults, beaked redfish appeared to concentrate more toward the central west of the Barents Sea, closer the continental slope, and were mostly absent in the eastern half of the Barents Sea. Adult beaked redfish also seemed to have the smallest distribution range.

On average, juvenile cod made up 87% of the total annual cod catches, peaking at a high of 97% in 1986 and 1987 and a low of 62% in 2013. The age structure of the catches of haddock was similar to that of cod, with juveniles (age < 6) making up on average 86% of the total annual catches, with a high of 99% and a low of 64% also on 1986 and 1987 and 2013, respectively. Beaked redfish were only aged from 1992 to 2011, where juveniles (age < 11) accounted for 62% of all the catches on average, with a peak of 85% in 1999 and a low of 23% in 2007.

Patterns in the spatial autocorrelation of fluctuations in abundance

At the population level, cod and haddock showed high degrees of spatial autocorrelation over very long distances, while beaked redfish showed long scaling of autocorrelation ($l = 365.1$ [median], 262.2–492.7 km [95% confidence interval]) but little or no synchrony over infinity ($\rho_\infty = 0.00, 0.12\text{--}0.00$; Fig. 2). The scaling of autocorrelation of cod ($l = 139.9, 123.5\text{--}159.6$ km) was on average longer than that of haddock ($l = 127.4, 107.9\text{--}150.3$ km). However, haddock showed a higher degree of autocorrelation at infinite distance ($\rho_\infty = 0.35, 0.30\text{--}0.40$) compared with cod ($\rho_\infty = 0.22, 0.14\text{--}0.30$) and beaked redfish. On average, haddock was the most spatially autocorrelated population, despite having the shortest spatial scaling. The high degree of autocorrelation at infinite distance in haddock and cod suggested that important autocorrelating mechanisms acted across the entire populations.

The patterns of spatial autocorrelation changed between the life stages of cod and beaked redfish, but not of haddock (Fig. 2). However, spatial autocorrelation increased with age in cod, while it decreased with age in beaked redfish. In cod, the increase in autocorrelation from juveniles (J) to adults (A) was evident at very long distances of separation ($\rho_{\infty,J} = 0.22, 0.13\text{--}0.30 < \rho_{\infty,A} = 0.44, 0.39\text{--}0.48$). In addition, in cod, negligible between-life stages variation was found in the spatial scaling of autocorrelation and in the autocorrelation at distances approaching zero. In contrast, the reduction in spatial autocorrelation from the juvenile to the adult stage of beaked redfish was mainly observed in the spatial scaling of autocorrelation ($l_J = 430.3, 319.9\text{--}602.5 > l_A = 119.5, 65.4\text{--}542.7$) and in the degree of autocorrelation at distances approaching zero ($\rho_{0,J} = 0.64, 0.59\text{--}0.69 > \rho_{0,A} = 0.42, 0.27\text{--}0.66$), while the degree of autocorrelation at infinity was close to zero in both stages ($\rho_{\infty,J} = 0.00, 0.00\text{--}0.00$; $\rho_{\infty,A} = 0.08, 0.00\text{--}0.28$).

The spatial autocorrelation of the cod population as a whole was almost identical to the pattern recorded in juveniles. In contrast, the degree of spatial autocorrelation of beaked redfish was closer to the average between the autocorrelations of either life stage, which might also be related to the more even representation of individuals from both life stages in the population. Despite the contraction of the geographical distribution of haddock with increasing age (Fig. 1a), the spatial autocorrelation of their density remained almost identical across life stages (Fig. 2). The degree of autocorrelation of the total haddock population was also almost identical to the autocorrelations of both life stages.

Cod age-specific autocorrelation

The patterns of spatial autocorrelation of individual age classes reflected in detail the gradual transition between the autocorrelation patterns from juveniles to

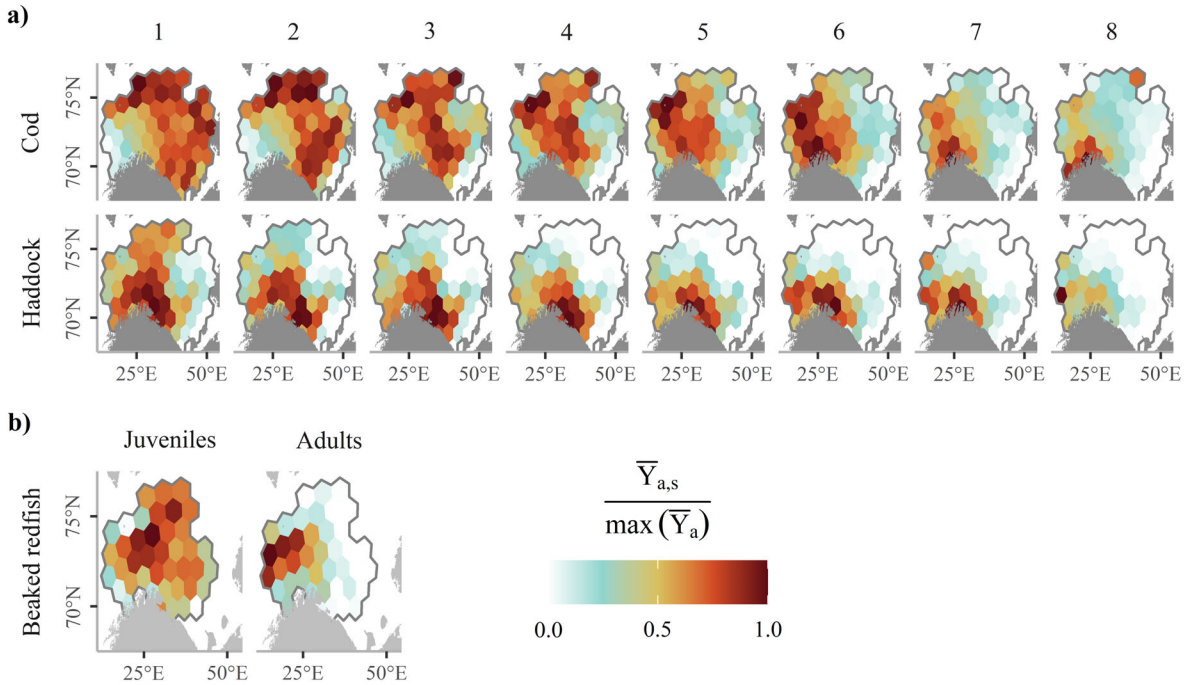


FIG. 1. Map of the study region, the Barents Sea, overlaid with the hexagonal grid used to average local densities. Here, the color of each cell indicates the average log-transformed density of that cell during the entire study period, divided by the value of the cell with the maximum average. Each column corresponds to an age (a) or life stage (b), while each row corresponds to the species marked on the left. The life stages are separated at the age at which 50% are on average mature in beaked redfish, i.e. juveniles include age classes <11 and adults include age classes ≥ 11 (ICES 2020). The black line around the colored hexagon cells represents the area in which individuals from that species have been caught.

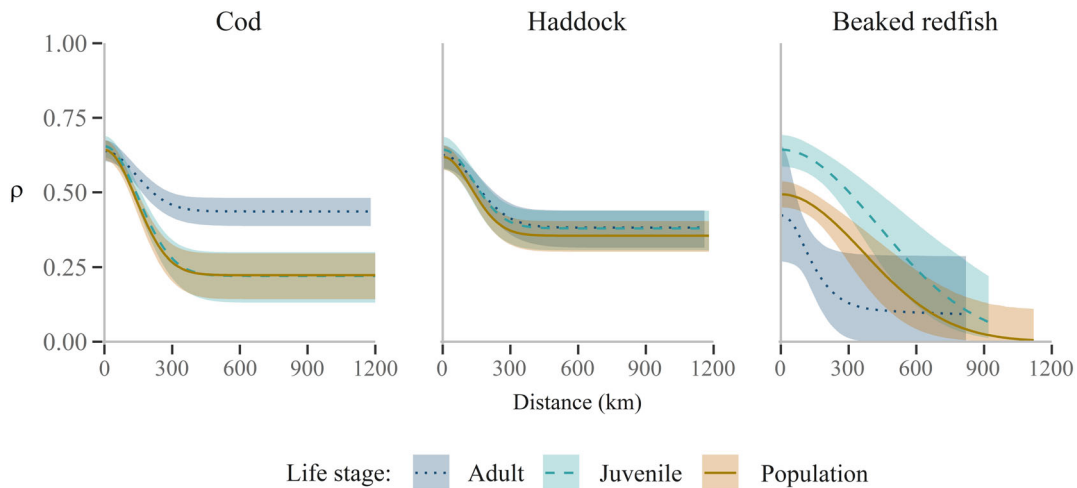


FIG. 2. Plots describing the decay of autocorrelation in density (ρ in the y-axis) with increased distance (x-axis) for each of the studied species (corresponding label at the top of each plot). The green dashed lines represent the spatial autocorrelation of the population density, while the solid dark and light blue lines represent the autocorrelation of the density of juveniles and adults, respectively. Smoother represent the 95% intervals obtained from the parametric bootstrap analyses. Juveniles refer to individual below the age at which 50% are on average mature, that is age 7 for cod, age 6 for haddock, and age 11 for beaked redfish (ICES 2020).

adults in cod and haddock (Fig. 3). The increase in ρ_∞ that characterized the transition in the spatial autocorrelation of juvenile to adult cod started to appear after age 5 ($\rho_\infty = 0.09, 0.00-0.20$), the age at which some

individuals start to reach maturity (ICES 2020), and increased gradually with each age class (Fig. 3c; age 6 $\rho_\infty = 0.20, 0.11-0.28$; age 7 $\rho_\infty = 0.28, 0.22-0.34$; age 8 $\rho_\infty = 0.36, 0.00-0.42$). In addition, age 1 cod showed a

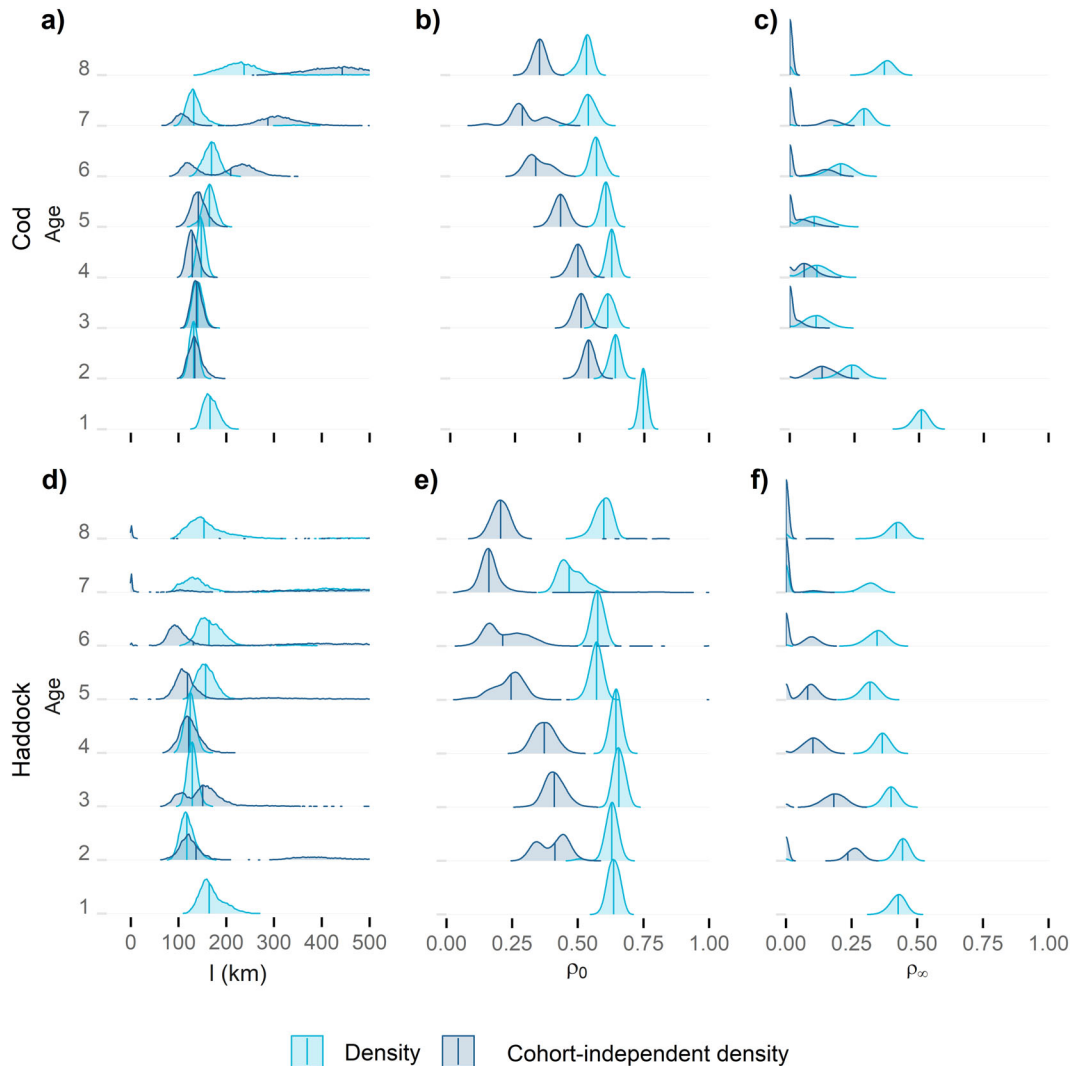


FIG. 3. Density distributions of the bootstraps of each of the key spatial autocorrelation parameters: scale of spatial autocorrelation (a, d), degree of autocorrelation at 0 distance (b, e), and degree of autocorrelation at infinite distance (c, f). The blue distributions correspond with the spatial autocorrelation estimates of the density of each age class. The darker blue distributions correspond with the spatial autocorrelation estimates of the density that is unexplained by the local cohort distribution during the previous year, i.e. cohort-independent distribution. The vertical lines within each of the distributions indicate the median value.

high ρ_∞ (0.51, 0.45–0.56) compared with the other studied age classes, which increased the overall degree of autocorrelation of the juvenile life stage. The scaling of autocorrelation did not vary among age classes, as expected based on the life stage results (Fig. 3a). However, while ρ_0 was also not expected to vary among age classes, the median ρ_0 estimates decreased gradually with age (median ρ_0 of ages 1–8 in order: $0.75 > 0.63 > 0.61 < 0.62 > 0.60 > 0.56 > 0.53 > 0.52$; Fig. 3b). Accounting for the expected effects of previous local cohort densities on current local cohort densities, i.e. cohort-independent density, resulted in lower degrees of autocorrelation among all age classes (Figs. 3b, c, 4b, c). At long distances, cohort-independent density showed little or no autocorrelation (median ρ_∞ of age classes 3–8

was < 0.05 , with lower 95% confidence interval of 0.00 and upper boundaries ranging from 0.07 to 0.20). This strongly suggested that local cohort dynamics enhanced spatial autocorrelation, especially among older age classes and at long distances. Accounting for local cohort dynamics did not affect the spatial scaling of the juvenile age classes of cod, but it increased the spatial scaling of the adult age classes, and its uncertainty (Fig. 4a).

Haddock age-specific autocorrelation

Spatial autocorrelations in abundance did not vary significantly or in a consistent way between the age classes of haddock, as expected based on the results from the analyses on life stages (Fig. 3d, e, f). However,

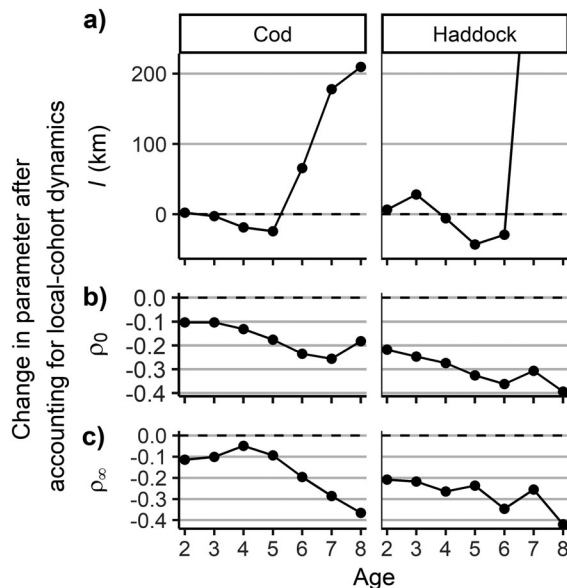


FIG. 4. Change in the median of the spatial autocorrelation parameters by age after accounting for the effect of local cohort dynamics: spatial scaling (a), degree of correlation as distance approaches 0 (b), and degree of correlation as distance approaches infinity (c). The change in spatial scaling of haddock's age classes 7 and 8 after accounting for local cohort dynamics were 578 and 2,131 km, respectively, but were left out to emphasize visually the variation in the other age classes.

the spatial autocorrelation of cohort-independent density did vary among age classes. Accounting for local cohort dynamics resulted in lower degrees of autocorrelation across all distances of separation (Fig. 4b, c). However, this reduction was more pronounced among the older age classes. The ρ_∞ estimates of haddock's cohort-independent density declined gradually with age (Fig. 3f; age 2 $\rho_\infty = 0.23$, 0.00–0.30; age 3 $\rho_\infty = 0.18$, 0.00–0.26; age 4 $\rho_\infty = 0.10$, 0.00–0.17; age 5 $\rho_\infty = 0.08$, 0.00–0.14), before becoming almost zero at age class 6. These results suggested that local cohort dynamics significantly influence the spatial autocorrelation patterns of cod and haddock, especially among older age classes (Fig. 4). For the values of all spatial autocorrelation parameters and ages, see Appendix S1: Figs. S1, S3.

DISCUSSION

Our study shows that spatial autocorrelation in density varies between the age classes of some species. Furthermore, the patterns differ among species because, within the Barents Sea, spatial autocorrelation increases among older age classes in cod, decreases among older age classes in beaked redbfish, and is constant among age classes in haddock (Fig. 5). These contrasting patterns suggest that the variation in spatial autocorrelation is not only related to age or age covariates like size (Hsieh et al. 2008, 2010, Ciannelli et al. 2013, Kuo et al. 2016, Wang et al. 2020), and that life strategy differences

among the species are likely to play an important role. Processes affecting autocorrelation, such as dispersal behavior (Paradis et al. 1999), strength and source of density regulation (Engen 2017), trophic interactions (Jarillo et al. 2020), or habitat preference (Bellamy et al. 2003), are known to vary distinctively between the age classes of our study species (Olsen et al. 2010). In addition, we showed that the autocorrelation patterns of older age classes of cod and haddock were increasingly related to the density distribution of the cohort in the previous year. This result is in line with our expectations, as older individuals are expected to become more resistant to adverse conditions and have better knowledge of, and preferential access to, optimal foraging grounds (Hsieh et al. 2010, Huse 2016). Our findings support the notion that changes in age structure can alter the spatio-temporal variance in the distribution of some species, as proposed by other studies (Hsieh et al. 2008, 2010, Cianelli et al. 2013, Kuo et al. 2016, Wang et al. 2020). Identifying how spatial autocorrelation varies among the life stages of a population can help us to better understand the causes of variation in spatial autocorrelation, and to better predict how population autocorrelation will change under changing environmental conditions (Benton et al. 2001).

Weaker density regulation in cod compared with haddock (Bjørkvoll et al. 2012) is likely to influence the longer spatial scaling of the autocorrelation in the fluctuations of the cod population (Marquez et al. 2019). This is because under weaker density regulation, individuals are expected to be less hindered by local density regulation, allowing them to disperse more, spreading the effects of local impacts, and therefore increasing spatial autocorrelation (Lande et al. 1999). Despite this, haddock showed a higher degree of autocorrelated population fluctuations over very long distances than cod. Age segregation in the cod population (Olsen et al. 2010) could help to explain its low degree of autocorrelation at long distances. Age-segregated populations are likely to experience different environmental conditions during different life stages depending on the local conditions of each stage, and could result in differences in their spatial autocorrelation patterns (Walter et al. 2017). In particular, young cod aggregate around the Polar front, a region where both cold Arctic currents and warm Atlantic currents meet, resulting in a highly heterogeneous environment with high productivity but temperatures that fluctuate around the lower limit of cod's thermal tolerance (Loeng and Drinkwater 2007). These highly stochastic and stressful environmental conditions, coupled with strong predation pressure, have important effects on the local dynamics of young cod, and could spatially decorrelate their density dynamics over long distances. Older cod gradually shift their range toward the southern and western Barents Sea where a warmer and more stable environment is likely to favor more stable density dynamics (Michalsen et al. 1998).

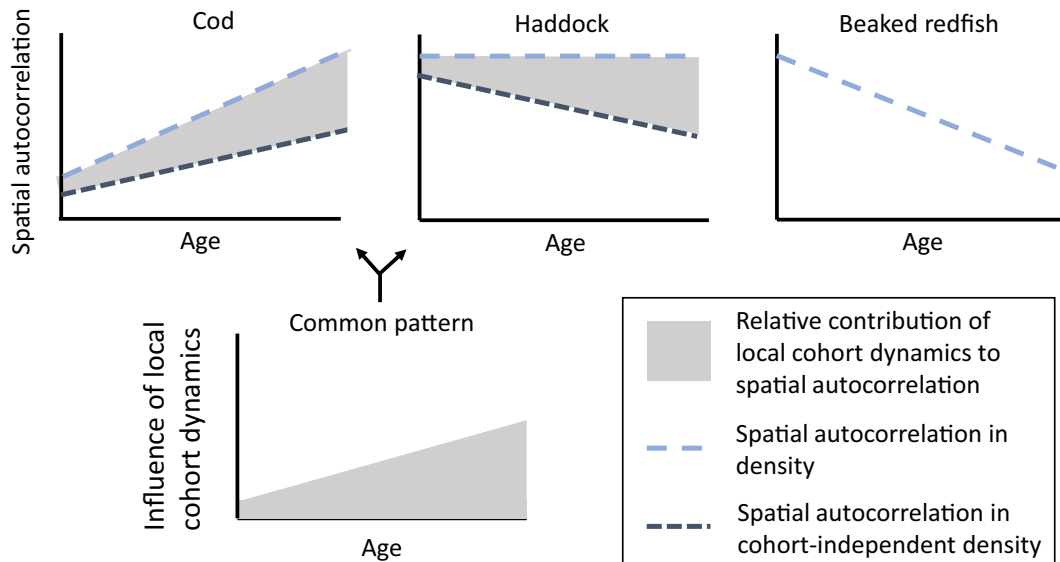


FIG. 5. Diagram summarizing the general patterns of variation in spatial autocorrelation with increased age for each of the study species. The bottom plot highlights the increased influence of local cohort dynamics on the spatial autocorrelation of older cod and haddock. Beaked redfish is missing information about cohort-dependent/-independent dynamics because data limitations prevented us from obtaining reliable results from the population.

Cannibalism by older individuals is one of the reasons for the age segregation in the cod population and this is expected to have several consequences for their spatial autocorrelation (Fogarty et al. 2001, Bogstad et al. 2016). We found that local cohort dynamics have little influence on the spatial autocorrelation patterns of younger cod, meaning that previous local cohort density was not a strong predictor of current local cohort density. As smaller individuals can be predated by larger conspecifics (Ciannelli et al. 2007), the cohort dynamics of consecutive years can become locally decoupled. In addition, if young cod are mostly absent in the environmentally favorable western Barents Sea because of predation by conspecifics (Ciannelli et al. 2007), a reduction in the abundance of older age classes might favor a greater presence of younger cod farther west, where more stable environmental conditions could possibly increasing overall spatial autocorrelation of the juvenile life stage. Conversely, although older cod tends to avoid the colder eastern Barents Sea, especially during colder years, an increase in the mean age of the population, as has been reported in recent years (ICES 2020), may result in an eastward expansion in their distribution, in turn restricting the distribution of younger age classes farther eastward into the Polar front region, where stochastic environmental conditions could reduce the spatial autocorrelation (Michalsen et al. 1998). Other mechanisms that might influence the increase in spatial autocorrelation with age in cod might relate to vertical social learning of optimal foraging areas from older to younger individuals (Huse 2016) or dispersal related to the annual spawning migrations of mature

individuals (Sundby and Nakken 2008, Olsen et al. 2010). After these migrations, individuals might redistribute across the Barents Sea in a way that spatially homogenizes local densities, increasing the degree of autocorrelation over long distances. In contrast, the degree of autocorrelation over short distances decreased with age in cod, which was unexpected. Perhaps this decrease is caused by the intense fishing pressure put on the older age classes (Engen et al. 2018a), however additional data would be needed to test this or alternative hypotheses.

Haddock's affinity for the south and southwestern waters of the Barents Sea was consistent across ages. Accordingly, and contrary to cod, haddock is expected to experience more similar environment conditions across life stages (Landa et al. 2014), possibly explaining the lack of among-age variation in spatial autocorrelation. However, the biology of the fish change throughout their lives so that, even if the environment is the same throughout life, different individuals are expected to experience it differently. For example, younger/smaller individuals can be expected to disperse at different rates and to be more sensitive to the environment and predation, which could have led to different autocorrelation patterns. This was not the case. In fact, haddock is reportedly less responsive to short-term environmental variability, not always adopting an ideal free distribution that would maximize resource allocation and optimal environmental conditions (Hidink et al. 2005, Landa et al. 2014). Despite this, the population dynamics of haddock were highly autocorrelated over very long distances, suggesting that a far-

reaching autocorrelating process exists. Widely autocorrelated environmental factors (e.g. sea temperature) are possible causes for this pattern, especially during the younger life stages, when individuals tend to be more vulnerable to adverse environments. In addition, similar to adult cod, the spawning migrations carried out by adult haddock could provide an opportunity to redistribute homogeneously across the Barents Sea, thereby increasing their degree of spatial autocorrelation of abundance (Olsen et al. 2010).

Diet differences have been previously used to explain differences in the spatial dynamic patterns of cod and haddock. Cod has a fish-based diet, while haddock feeds more on benthic organisms (Burgos and Mehl 1987). Because fish can respond faster to environmental changes than can benthic organisms, through higher dispersal potential, cod might need to adapt their spatial distribution more rapidly, reducing their spatial autocorrelation. In contrast, haddock's benthic prey is likely to remain more spatially constrained, having a lesser impact on the spatio-temporal dynamics of haddock (Landa et al. 2014). In addition, although the spatial autocorrelation was consistent among the age classes of haddock, the spatial autocorrelation in the cohort-independent density decreased with age. This means that, especially among older age classes of haddock, the local density of a cohort in one year is a strong predictor for their local density the following year, suggesting a strong geographic attachment or homing behavior. Haddock's benthic diet favors territorial or homing behavior in which individuals remain or return to familiar grounds to search for food under the sediments, instead of testing new regions (Gjøsæter 2009). Previous studies have also suggested that the distribution of haddock might be more cohort dependent than age dependent, which could also explain our results (Mehl et al. 2016).

Beaked redfish has a slower life history (i.e. lower population growth at small population sizes, higher survival, lower fecundity, and a longer generation time) than the other two study species (Bjørkvoll et al. 2012). Because of this, and because it forages in deeper waters where the environmental conditions tend to be more stable, the higher scaling of autocorrelation observed in beaked redfish was expected (Marquez et al. 2019). However, the high degree of spatial autocorrelation was mostly associated with the pattern observed among juveniles. The distribution of adult beaked redfish showed low spatial autocorrelation and was highly concentrated into a small region near the continental slope of the central western Barents Sea. Commercial catches of beaked redfish indicated that a proportion of the adult population is also distributed in the open ocean, outside our study area (ICES 2020). We might therefore be capturing the spatial autocorrelation pattern of adult beaked redfish within the Barents Sea, but not across its entire range. Another major distinguishing characteristic of beaked redfish which might influence the lack of spatial autocorrelation in the adult stage is that they are

ovoviviparous species (i.e. eggs are fertilized and hatch internally, and larvae are later extruded by the females). While the sexes meet to copulate in autumn, the sexes might segregate during the sampling period, as females migrate toward the continental slope to extrude the larvae, potentially influencing the observed pattern (Drevetnyak et al. 2011, Planque et al. 2011, 2013). As with age segregation, sex segregation might lead to different spatial autocorrelation patterns for each of the sexes and might interfere with the detection of a general spatial autocorrelation pattern encompassing the mature stage (Saborido-Rey et al. 2010). Unfortunately, no sex-specific spatial data were available to examine this hypothesis.

We have suggested several potential processes that could be responsible for the variations in spatial autocorrelation between ages. The current study did not allow us to test and disentangle the relative importance of these processes. However, we suggest that an important future step for this field of research will be to test and quantify such effects using environmental and/or multispecies data. In addition, given the data used, our results are representative of the spatial dynamics of the study species within the Barents Sea and during the winter months. As some fish spatial dynamics can vary between different life events (e.g. spawning, migrations, foraging; Nøttestad et al. 1996), future studies on the seasonality in spatial autocorrelation patterns could help us to disentangle additional autocorrelation processes. Understanding the processes that cause spatial autocorrelation in fluctuations among geographically separated locations is important for conservation and harvesting, because spatial autocorrelation affects crucial ecological processes such as population sensitivity to environmental changes (Hanski and Woiwod 1993), disease outbreaks, invasive species (Ovaskainen and Cornell 2006), maximum sustainable yield (Lee et al. 2017, Engen et al. 2018a, Jarillo et al. 2020), or the probability of extinction (Heino et al. 1997, Engen et al. 2002a). Similarly, fluctuations in age-distributions strongly affect temporal variation in population size (Anderson et al. 2008), but our understanding of how spatial autocorrelation and age structure interact is limited. We have shown that the spatial autocorrelation of abundance varies among age classes on three marine fish species in species-specific ways. As changes to the age structure of some species' populations could alter their spatial autocorrelation, managers should consider the potential indirect effects associated with different spatial autocorrelation patterns when altering age structures through harvesting. As the importance of spatial population dynamics becomes increasingly recognized (Thorson et al. 2015, Hansen et al. 2020), and better and more diverse spatial data are more increasingly collected, future studies should strive to disentangle the individual processes that cause spatial patterns to improve predictions of population dynamics and distributions in the constantly changing environment.

ACKNOWLEDGMENTS

We thank all the people in the Russian Polar Research Institute of Marine Fisheries and Oceanography and the Norwegian Institute of Marine Research that put immense effort in collecting the data used in our research. We also want to thank Vidar Grøtan and Stefan Vriend for helpful discussions and comments on an earlier draft, and three anonymous reviewers for providing valuable comments to the manuscripts. This study was funded by the Research Council of Norway through the Centre of Excellence Centre for Biodiversity Dynamics (project 223257) and research project SUSTAIN (244647).

LITERATURE CITED

- Aanes, S., and J. H. Vølstad. 2015. Efficient statistical estimators and sampling strategies for estimating the age composition of fish. *Canadian Journal of Fisheries and Aquatic Sciences* 72:938–953.
- Albikovskaya, L. K., and O. V. Gerasimova. 1993. Food and feeding patterns of cod (*Gadus morhua* L.) and beaked redfish (*Sebastes mentella* Travin) on Flemish Cap. *NAFO Scientific Council Studies* 19:31–39.
- Anderson, C. N. K., C. H. Hsieh, S. A. Sandin, R. Hewitt, A. Hollowed, J. Beddington, R. M. May, and G. Sugihara. 2008. Why fishing magnifies fluctuations in fish abundance. *Nature* 452:835–839.
- Bellamy P. E., P. Rothery, and S. A. Hinsley. 2003. Synchrony of woodland bird populations: the effect of landscape structure. *Ecography* 26:338–348.
- Benton, T. G., C. T. Lapsley, and A. P. Beckerman. 2001. Population synchrony and environmental variation: an experimental demonstration. *Ecology Letters* 4:236–243.
- Berkeley, S. A., M. A. Hixon, R. J. Larson, and M. S. Love. 2004. Fisheries sustainability via protection of age structure and spatial distribution of fish populations. *Fisheries* 29:23–32.
- Bjørkvoll, E., V. Grøtan, S. Aanes, B.-E. Sæther, S. Engen, and R. Aanes. 2012. Stochastic population dynamics and life-history variation in marine fish species. *American Naturalist* 180:372–387.
- Bogstad, B., N. A. Yaragina, and R. D. M. Nash. 2016. The early life-history dynamics of Northeast Arctic cod: levels of natural mortality and abundance during the first 3 years of life. *Canadian Journal of Fisheries and Aquatic Sciences* 73:146–256.
- Burgos, G., and S. Mehl. 1987. Diet overlap between Northeast Arctic cod and haddock in the southern part of the Barents Sea in 1984–1986. *ICES CM documents* G:50.
- Ciannelli, L., G. E. Dingsør, B. Bogstad, G. Ottersen, K. S. Chan, H. Gjøsæter, J. E. Stiansen, and N. C. Stenseth. 2007. Spatial anatomy of species survival: effects of predation and climate-driven environmental variability. *Ecology* 88:635–646.
- Ciannelli, L., J. A. D. Fisher, M. Skern-Mauritzen, M. E. Hunsicker, M. Hidalgo, K. T. Frank, and K. M. Bailey. 2013. Theory, consequences and evidence of eroding population spatial structure in harvested marine fishes: a review. *Marine Ecology Progress Series* 480:227–243.
- Dalpadado, P., B. Bogstad, E. Eriksen, and L. Rey. 2009. Distribution and diet of 0-group cod (*Gadus morhua*) and haddock (*Melanogrammus aeglefinus*) in the Barents Sea in relation to food availability and temperature. *Polar Biology* 32:1583–1596.
- Dolgov, A., E. Johannesen, and B. Bogstad. 2011. An overview of trophic interactions in the Barents Sea. Pages 455–465 in T. Jakobsen and V. Ozhigin, editors. *The Barents Sea – ecosystem, resources, management. Half a century of Russian-Norwegian cooperation*. Tapir Academic Press, Trondheim, Norway.
- Drevetnyak, K. H., K. H. Nedreaas, and B. Planque. 2011. Beaked redfish. Pages 292–307 in T. Jakobsen and V. K. Ozhigin, editors. *The Barents Sea, ecosystem, resources, management. Half a Century of Russian–Norwegian cooperation*. Tapir Academic Press, Trondheim, Norway.
- Engen, S. 2017. Spatial synchrony and harvesting in fluctuating populations: Relaxing the small noise assumption. *Theoretical Population Biology* 116:18–26.
- Engen, S., F. J. Cao, and B.-E. Sæther. 2018a. The effect of harvesting on the spatial synchrony of population fluctuations. *Theoretical Population Biology* 123:28–34.
- Engen, S., R. Lande, and B.-E. Sæther. 2002a. The spatial scale of population fluctuations and quasi-extinction risk. *American Naturalist* 160:439–451.
- Engen, S., R. Lande, B.-E. Sæther, and T. Bregnballe. 2005. Estimating the pattern of synchrony in fluctuating populations. *Journal of Animal Ecology* 74:601–611.
- Engen, S., R. Lande, T. Walla, and P. J. DeVries. 2002b. Analyzing spatial structure of communities using the two-dimensional poisson lognormal species abundance model. *American Naturalist* 160:60–73.
- Engen, S., A. M. Lee, and B.-E. Sæther. 2018b. Spatial distribution and optimal harvesting of an age-structured population in a fluctuating environment. *Mathematical Biosciences* 296:36–44.
- Engen, S., and B.-E. Sæther. 2005. Generalizations of the Moran effect explaining spatial synchrony in population fluctuations. *American Naturalist* 166:603–612.
- Fall, J. E. et al. 2020. Fish investigations in the Barents Sea winter 2020.
- Fogarty, M. J., R. A. Myers, and K. G. Bowen. 2001. Recruitment of cod and haddock in the North Atlantic: a comparative analysis. *ICES Journal of Marine Science* 58:952–961.
- Gamelon, M., V. Grøtan, S. Engen, E. Bjørkvoll, M. E. Visser, and B.-E. Sæther. 2016. Density dependence in an age-structured population of great tits: Identifying the critical age classes. *Ecology* 97:2479–2490.
- Gjøsæter, H. 2009. Commercial fisheries (fish, seafood and marine mammals). Pages 373–413 in E. Sakshaug, G. Johnsen, and K. Kovacs, editors. *Ecosystem Barents Sea*. Tapir Academic Press, Trondheim, Norway.
- Grøtan, V., B.-E. Sæther, S. Engen, E. J. Solberg, J. D. Linnell, R. Andersen, H. Broseth, and E. Lund. 2005. Climate causes large-scale spatial synchrony in population fluctuations of a temperature herbivore. *Ecology* 86:1472–1482.
- Hansen, B. B., V. Grøtan, I. Herfjndal, and A. M. Lee. 2020. The Moran effect revisited: spatial population synchrony under global warming. *Ecography* 43:1591–1602.
- Hanski, I., and I. P. Woiwod. 1993. Spatial synchrony in the dynamics of moth and aphid populations. *Journal of Animal Ecology* 62:656.
- Heino, M., V. Kaitala, E. Ranta, and J. Lindström. 1997. Synchronous dynamics and rates of extinction in spatially structured populations. *Proceedings of the Royal Society of London B: Biological Sciences* 264:481–486.
- Hiddink, J. G., S. Jennings, and M. J. Kaiser. 2005. Do haddock select habitats to maximize condition? *Journal of Fish Biology* 67:111–124.
- Hsieh, C. H., C. S. Reiss, R. P. Hewitt, and G. Sugihara. 2008. Spatial analysis shows that fishing enhances the climatic sensitivity of marine fishes. *Canadian Journal of Fisheries and Aquatic Sciences* 65:947–961.

- Hsieh, C.-H., A. Yamauchi, T. Nakazawa, and W.-F. Wang. 2010. Fishing effects on age and spatial structures undermine population stability of fishes. *Aquatic Sciences* 72:165–178.
- Huse, G. 2016. A spatial approach to understanding herring population dynamics. *Canadian Journal of Fisheries and Aquatic Sciences* 73:177–188.
- ICES. 2019. Barents Sea Ecoregion – Ecosystem overview. *in* Report of the ICES Advisory Committee, 2019. ICES Advice 2019 5.1. ICES.
- ICES. 2020. Arctic Fisheries Working Group (AFWG). ICES Scientific Reports. 2:52. 577 pp.
- Ims, R. A., and H. P. Andreassen. 2000. Spatial synchronization of vole population dynamics by predatory birds. *Nature* 408:194–196.
- Jakobsen, T., K. Korsbrekke, S. Mehl, and O. Nakken. 1997. Norwegian combined acoustic and bottom trawl surveys for demersal fish in the Barents Sea during winter. *ICES* 17:26.
- Jarillo, J., B.-E. Sæther, S. Engen, and F. J. Cao-Garcia. 2020. Spatial scales of population synchrony in predator-prey systems. *American Naturalist* 195:216–230.
- Jenkins, D. G., et al. 2007. Does size matter for dispersal distance? *Global Ecology and Biogeography* 16:415–425.
- Johannesen, E., T. D. L. Wenneck, Å. Høines, A. Aglen, S. Mehl, H. Mjanger, Å. Fotland, T. Ivar, and T. Jakobsen. 2009. Egner vintertoktet seg til overvåking av endringer i fiskesamfunnet i Barentshavet?: en gjennomgang av metodikk og data fra 1981–2007 (Can the winter survey be used to detect changes in the Barents Sea fish community? - An overview of methods and data fr. Page Fisken og havet. Bergen, Norway.
- Kuo, T. C., S. Mandal, A. Yamauchi, and C. H. Hsieh. 2016. Life history traits and exploitation affect the spatial mean-variance relationship in fish abundance. *Ecology* 97:1251–1259.
- Landa, C. S., G. Ottersen, S. Sundby, G. E. Dingsør, and J. E. Stiansen. 2014. Recruitment, distribution boundary and habitat temperature of an arcto-boreal gadoid in a climatically changing environment: a case study on Northeast Arctic haddock (*Melanogrammus aeglefinus*). *Fisheries Oceanography* 23:506–520.
- Lande, R., S. Engen, and B.-E. Sæther. 1999. Spatial scale of population synchrony: environmental correlation versus dispersal and density regulation. *American Naturalist* 154:271–281.
- Lee, A. M., B.-E. Sæther, S. S. Markussen, and S. Engen. 2017. Modelling time to population extinction when individual reproduction is autocorrelated. *Ecology Letters* 20:1385–1394.
- Liebold, A., W. D. Koenig, and O. N. Bjørnstad. 2004. Spatial synchrony in population dynamics. *Annual Review of Ecology, Evolution, and Systematics* 35:467–490.
- Lindström, J., and H. Kokko. 2002. Cohort effects and population dynamics. *Ecology Letters* 5:338–344.
- Loeng, H., and K. Drinkwater. 2007. An overview of the ecosystems of the Barents and Norwegian Seas and their response to climate variability. *Deep Sea Research Part II: Topical Studies in Oceanography* 54:2478–2500.
- Marquez, J., S. Aanes, and A. Salthaug. 2021. Data and scripts used in "Age-dependent patterns of spatial autocorrelation in fish populations". Figshare, data set. <https://doi.org/10.6084/m9.figshare.14686683.v1>
- Marquez, J. F., A. M. Lee, S. Aanes, S. Engen, I. Herfindal, A. Salthaug, and B.-E. Sæther. 2019. Spatial scaling of population synchrony in marine fish depends on their life history. *Ecology Letters* 22:1787–1796.
- Mehl, S., A. Aglen, B. Bogstad, G. E. Dingsør, K. Korsbrekke, E. Olsen, A. Staby, T. D. L. Wenneck, R. Wienerroither, A. Amelkin, and A. Russkikh. 2016. Fish investigations in the Barents Sea winter 2016. IMR/PINRO Joint Report Series
- Michalsen, K., G. Ottersen, and O. Nakken. 1998. Growth of North-east Arctic cod (*Gadus morhua* L.) in relation to ambient temperature. *ICES Journal of Marine Science* 55:863–877.
- Mjanger, H., B. V. Svendsen, H. Senneset, E. Fuglebakk, M. L. Skage, J. Diaz, G. O. Johansen, and T. Vollen. 2020. Handbook for sampling fish, crustaceans and other invertebrates Version 2.0. 157 pp. Institute of Marine Research, Norway.
- Moran, P. 1953. The statistical analysis of the Canadian lynx cycle. II. Synchronization and meteorology. *Australian Journal of Zoology* 1:291–298.
- Nielsen, J. K., and A. C. Seitz. 2017. Interannual site fidelity of Pacific halibut: Potential utility of protected areas for management of a migratory demersal fish. *ICES Journal of Marine Science* 74:2120–2134.
- Nøttestad, L., M. Aksland, A. Beltestad, A. Fernö, A. Johannessen, and O. Arve Misund. 1996. Schooling dynamics of Norwegian spring spawning herring (*Clupea harengus* L.) in a coastal spawning area. *Sarsia* 80:277–284.
- Olsen, E., S. Aanes, S. Mehl, J. C. Holst, A. Aglen, and H. Gjøsæter. 2010. Cod, haddock, saithe, herring, and capelin in the Barents Sea and adjacent waters: a review of the biological value of the area. *ICES Journal of Marine Science* 67:87–101.
- Ovaskainen, O., and S. J. Cornell. 2006. Space and stochasticity in population dynamics. *Proceedings of the National Academy of Sciences of the United States of America* 103:12781–12786.
- Paradis, E., S. R. Baillie, W. J. Sutherland, and R. D. Gregory. 1999. Dispersal and spatial scale affect synchrony in spatial population dynamics. *Ecology Letters* 2:114–120.
- Planque, B., et al. 2013. Monitoring beaked redfish (*Sebastes mentella*) in the North Atlantic, current challenges and future prospects. *Aquatic Living Resources* 26:293–306.
- Planque, B., C. Loots, P. Petitgas, L. Ulf, and S. Vaz. 2011. Understanding what controls the spatial distribution of fish populations using a multi-model approach. *Fisheries Oceanography* 20:1–17.
- Quinn, T. J., and R. B. Deriso. 1999. Age-structured models: per-recruit and year-class models. Page 239 *in* W. M. Getz, editor. *Quantitative fish dynamics*. Oxford University Press, New York, New York, USA, Oxford, UK.
- R Core Team. 2020. R: A language and environment for statistical computing. R Foundation for Statistical Computing, Vienna, Austria.
- Reuman, D. C., L. Zhao, L. W. Sheppard, P. C. Reid, and J. E. Cohen. 2017. Synchrony affects Taylor's law in theory and data. *Proceedings of the National Academy of Sciences of the United States of America* 114 6788–6793.
- Saborido-Rey, F., et al. 2010. Population structure of beaked redfish, *Sebastes mentella*: evidence of divergence associated with different habitats. *ICES Journal of Marine Science* 67:1617–1630.
- Sundby, S., and O. Nakken. 2008. Spatial shifts in spawning habitats of Arcto-Norwegian cod related to multidecadal climate oscillations and climate change. *ICES Journal of Marine Science* 65:953–962.
- Tedesco, P. A., B. Hugueny, D. Paugy, and Y. Fermon. 2004. Spatial synchrony in population dynamics of West African fishes: a demonstration of an intraspecific and interspecific Moran effect. *Journal of Animal Ecology* 73:693–705.
- Thorson, J. T., H. J. Skaug, K. Kristensen, A. O. Shelton, E. J. Ward, J. H. Harms, and J. A. Benante. 2015. The importance of spatial models for estimating the strength of density dependence. *Ecology* 96:1202–1212.

- Vasseur, D. A., and J. W. Fox. 2009. Phase-locking and environmental fluctuations generate synchrony in a predator-prey community. *Nature* 460:1007–1010.
- Walter, J. A., L. W. Sheppard, T. L. Anderson, J. H. Kastens, O. N. Bjørnstad, A. M. Liebhold, and D. C. Reuman. 2017. The geography of spatial synchrony. *Ecology Letters* 20:801–814.
- Wang, J. Y., T. C. Kuo, and C.-H. Hsieh. 2020. Causal effects of population dynamics and environmental changes on spatial variability of marine fishes. *Nature Communications* 11:1–10.

SUPPORTING INFORMATION

Additional supporting information may be found in the online version of this article at <http://onlinelibrary.wiley.com/doi/10.1002/ecy.3523/suppinfo>

OPEN RESEARCH

Data and scripts (Marquez et al. 2021) are publicly archived in Figshare at: <https://doi.org/10.6084/m9.figshare.14686683.v1>.